

Introduction. Please refer to the main text for any definitions and references that are not stated here.

Text S1. As argued in the main text, the charge/discharge to the thermodynamic carrying capacity can be represented as

$$\frac{f(L_{\infty,h}) - f(L)}{\tau_t},$$

where L is the liquid water path, $L_{\infty,h}$ the thermodynamic carrying capacity, and τ_t the timescale of this process. However, the form of the function f is not known. In the main text, $f(x) = x$ is used, to which we refer to as linear thermodynamic charge/discharge. In this supplement, a logarithmic version in the form of $f(x) = \ln(x)$ is explored.

Using the same setup as for Fig. 2, Fig. S2 shows the sensitivity of the model with logarithmic thermodynamic charge/discharge to the model parameters (a) τ_t , (b) c_1 , (c) L_0 , and (d) $m_{\infty,h}$. Without addressing the details of each panel, one sees clearly that the model assumes the prescribed slope $m_{\infty,h}$ for high N as expected (thin red lines). For small N , however, the slope $m_1 = 0.43$ (thin black line) is larger than $m_{\infty,h}$ (thin blue lines). The reason for this is the faster logarithmic thermodynamic recharge of precipitation losses. While larger L at low N could be remedied with an increased precipitation constant c_1 (panel b), m_1 cannot be tuned to match $m_{\infty,h}$ and hence the ensemble LES results of Glassmeier et al. (2021). In fact, m_1 does not vary for $m_{\infty,h} < 2.0$ when logarithmic thermodynamic charge/discharge is used (panel d), indicating fundamental differences between the linear and logarithmic formulations. Based on this analysis, we find that linear thermodynamic charge/discharge agrees better with our reference (Glassmeier et al., 2021), and is thus used in this study.

Text S2. As stated in (3) of the main text, the temporal change of L is given by

$$\frac{dL}{dt} = \frac{L_{\infty,h} - L}{\tau_t} - c_1 \frac{L^{3/2}}{N}.$$

From the steady state solution of (3), we determine the derivative with respect to N as

$$0 = \frac{d}{dN} \left[\frac{L_{\infty,h} - L_{\infty}}{\tau_t} - c_1 \frac{L_{\infty}^{3/2}}{N} \right].$$

Solving for dL_{∞}/dN gives

$$\frac{dL_{\infty}}{dN} = \left(\frac{1}{\tau_t} \frac{dL_{\infty,h}}{dN} + c_1 \frac{L_{\infty}^{3/2}}{N^2} \right) \left(\frac{1}{\tau_t} + \frac{3}{2} c_1 \frac{L_{\infty}^{1/2}}{N} \right)^{-1}.$$

The slope m relates to dL/dN as

$$m = \frac{d \ln(L)}{d \ln(N)} = \frac{N}{L} \frac{dL}{dN}.$$

This yields for the steady state

$$m_{\infty} = \left(\frac{1}{\tau_t} \frac{N}{L_{\infty}} \frac{dL_{\infty,h}}{dN} + c_1 \frac{L_{\infty}^{1/2}}{N} \right) \left(\frac{1}{\tau_t} + \frac{3}{2} c_1 \frac{L_{\infty}^{1/2}}{N} \right)^{-1}.$$

Using definition (5), we determine that

$$\begin{aligned} \frac{N}{L_{\infty}} \frac{dL_{\infty,h}}{dN} &= \frac{N}{L_{\infty}} \frac{d}{dN} \left[L_0 \left(\frac{N}{N_0} \right)^{m_{\infty,h}} \right] \\ &= m_{\infty,h} \frac{L_{\infty,h}}{L_{\infty}} \\ &= m_{\infty,h} \left[1 + \frac{2}{3} \frac{\tau_t}{\tau_p} \right], \end{aligned}$$

where we used (7) for the last equality. With the definition of the precipitation timescale (4),

$$\tau_p = \frac{2}{3} \frac{1}{c_1} \frac{N}{L^{1/2}},$$

we find

$$m_\infty = \left(\frac{1}{\tau_t} m_{\infty, h} + \frac{1}{\tau_p} \frac{2}{3} (m_{\infty, h} + 1) \right) \left(\frac{1}{\tau_t} + \frac{1}{\tau_p} \right)^{-1}.$$

This expression can be rearranged to yield

$$m_\infty = \frac{m_{\infty, h}}{1 + \frac{\tau_t}{\tau_p}} + \frac{\frac{2}{3} (m_{\infty, h} + 1)}{1 + \frac{\tau_t}{\tau_p}},$$

which is (8) in the main text.

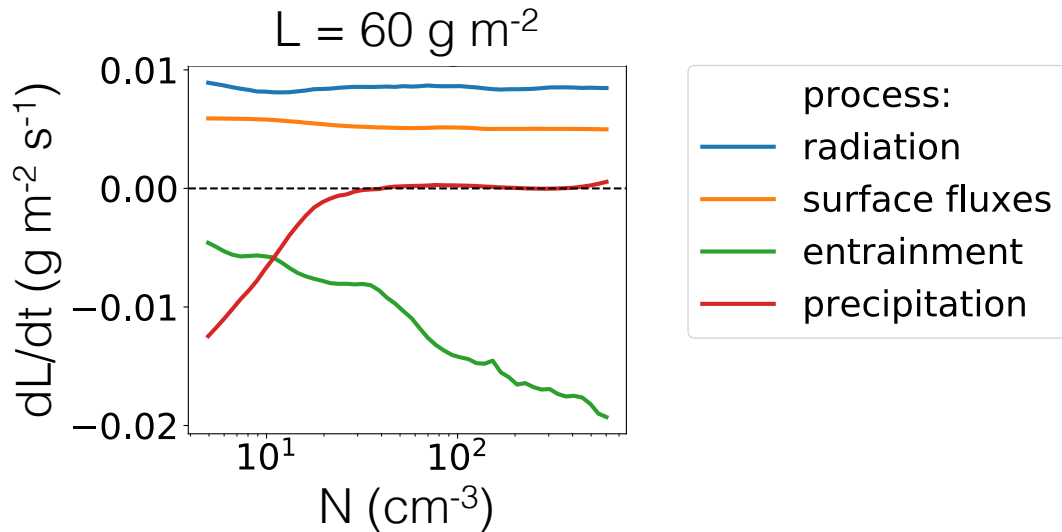


Figure S1. The temporal change of L as a function of N for thermodynamics [radiation (blue), surface fluxes (orange), and entrainment (green)] and precipitation (red) is shown for $L = 60 \text{ g m}^{-2}$. Note that this plot is based on the data shown in Fig. 3 of Hoffmann et al. (2020), but presented to fit the arguments of this study. Please refer to Hoffmann et al. (2020) for details on how this graph has been created.

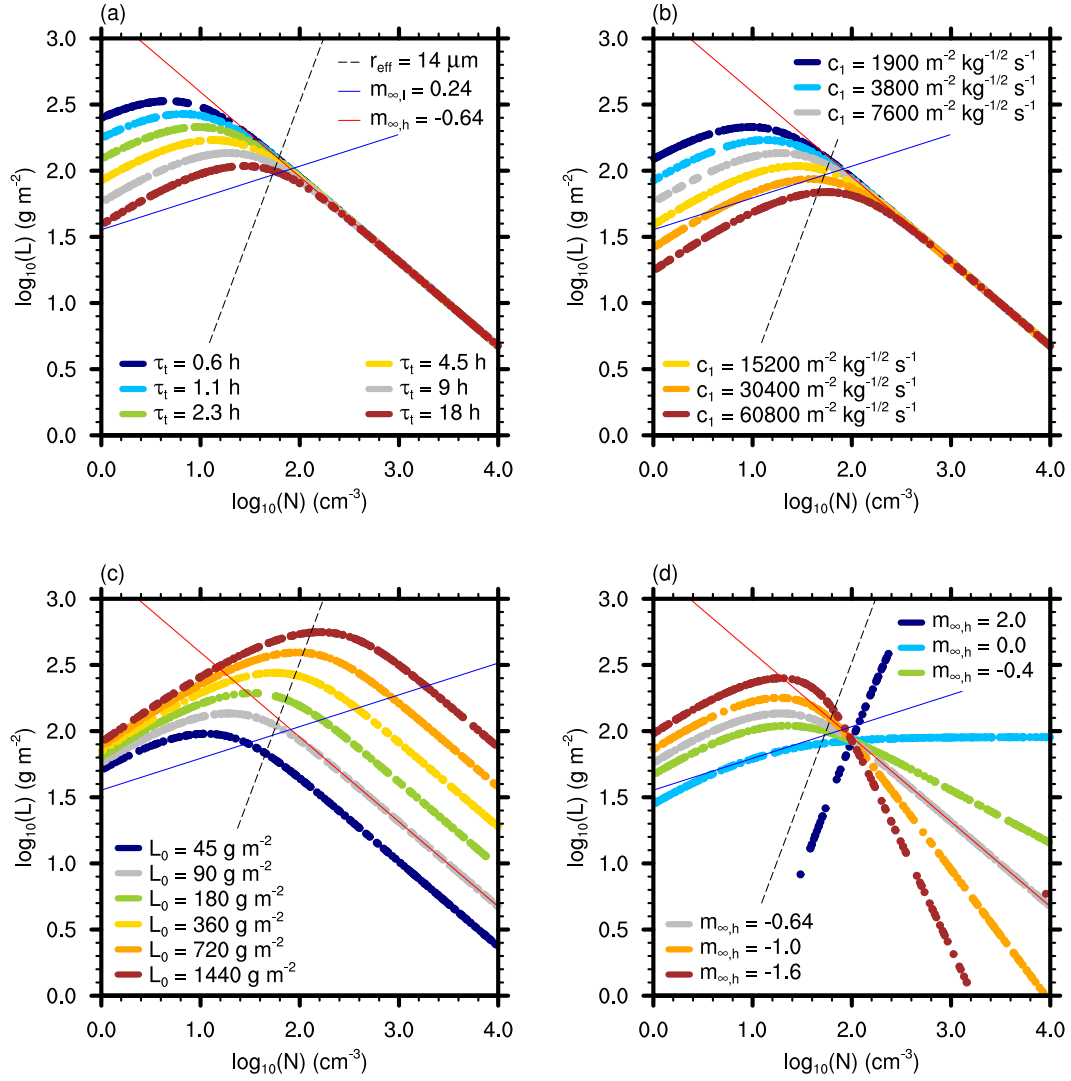


Figure S2. For a system with logarithmic thermodynamic charge/discharge, we show L after 7 days as a function of N for variations in (a) τ_t , (b) c_1 , (c) L_0 , and (d) $m_{\infty,h}$ (colored dots). The default configuration is differentiated by gray dots. Plots are overlaid with $m_{\infty,l} = 0.24$, $m_{\infty,h} = -0.64$, and $m_1 = 0.43$ (thin blue, red, and black lines, respectively), and the $14 \mu\text{m}$ cloud top effective droplet radius (black dashed line).

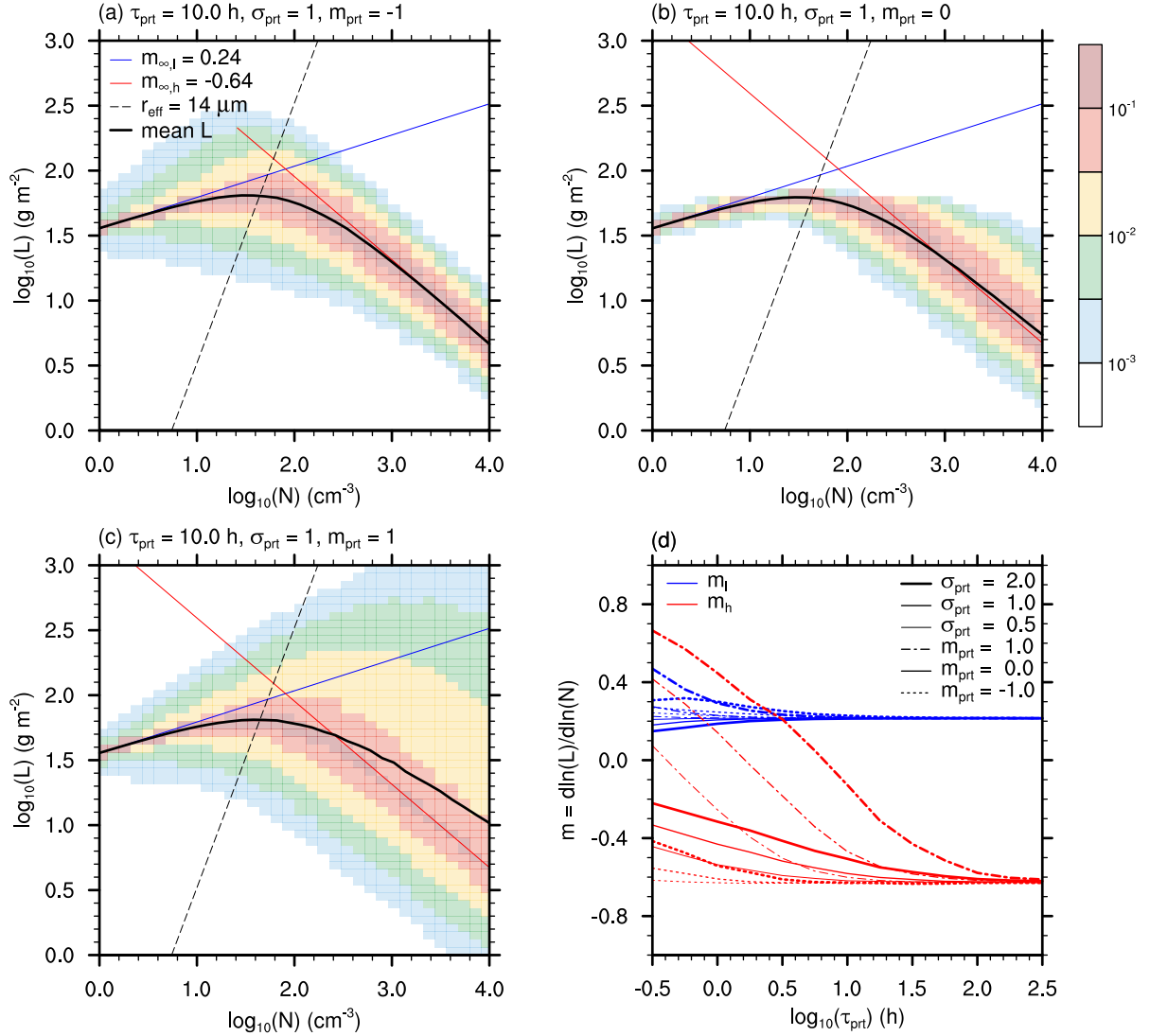


Figure S3. Joint L - N histograms (opaque colors) and mean $\ln(L)$ (thick black line) for perturbations in L and N for $\tau_{\text{prt}} = 10 \text{ h}$, $\sigma_{\text{prt}} = 1.0$ with (a) $m_{\text{prt}} = -1$, (b) 0.0 , and (c) 1.0 . Plots are overlaid with $m_{\infty,l} = 0.24$ and $m_{\infty,h} = -0.64$ (blue and red lines), and the $14 \mu\text{m}$ cloud top effective droplet radius (black dashed line). Note that the histograms are normalized such that the integral over each N column yields 1 (cf. Gryspeerdt et al., 2019). Panel (d) shows the fitted slopes m_l (blue lines) and m_h (red lines) for $\sigma_{\text{prt}} = 0.5$ (thin lines), 1.0 (medium lines), 2.0 (thick lines), and $m_{\text{prt}} = -1.0$ (dashed lines), 0.0 (continuous lines), 1.0 (dashdotted lines).